## Geodynamic Implications of Jurassic Ophiolites Associated with Island-Arc Volcanics, South Apuseni Mountains, Western Romania.

(Article begins on next page)

20 December 2021

# CONTENTS

Edited by

W. Gary Ernst                    Brian J. Skinner

# Geodynamic Implications of Jurassic Ophiolites Associated with Island-Arc Volcanics, South Apuseni Mountains, Western Romania

VALERIO BORTOLOTTI,

*Dipartimento di Scienze della Terra, Universita' di Firenze, 50122 Firenze, Italy*

MICHELE MARRONI,[1]

*Dipartimento di Scienze della Terra, Universita' di Pisa, 56126 Pisa, Italy*

IONEL NICOLAE,

*Romanian Academy Institute of Geodynamics, 79678 Bucuresti, Romania*

LUCA PANDOLFI,

*Consiglio Nazionale delle Ricerche, Istituto di Geoscienze e Georisorse, 56126 Pisa, Italy*

GIANFRANCO PRINCIPI,

*Dipartimento di Scienze della Terra, Universita' di Firenze, 50122 Firenze, Italy*

AND EMILIO SACCANI

*Dipartimento di Scienze della Terra, Università di Ferrara, 44100 Ferrara, Italy*

## Abstract

The South Apuseni Mountains are located in the inner zone of the Carpathian belt. This area is characterized by a complex assemblage of nappes, in which Jurassic igneous associations are well represented. New geological and geochemical data on these igneous associations document the occurrence of Middle Jurassic ophiolites overlain by Late Jurassic calc-alkaline volcanic rocks.

The ophiolite sequence is characterized by: (1) an intrusive section mainly represented by small gabbroic bodies showing both layered and isotropic textures, as well as scarce ultramafic cumulates, melagabbros, gabbronorites, and ferrogabbros; (2) a basaltic sheeted dike complex; (3) a volcanic sequence including massive and pillow-lava basalts and rare pillow breccias; and (4) very rare Callovian–Oxfordian radiolarian cherts. Although chemically variable, gabbros show a clear high-Ti magmatic affinity. Basaltic rocks display N-MORB–normalized incompatible-element patterns consistent with the compositions of present-day mid-ocean ridge basalts. Their high-Ti magmatic affinity is indicated by the chondrite-normalized REE patterns, which are rather flat or slightly enriched in light REE. All these features suggest that ophiolites of the South Apuseni Mountains were generated in a mid-ocean ridge setting. Evidence of ductile deformation and synkinematic metamorphism are lacking, suggesting that ophiolites were dismembered in multiple slices at shallow structural levels during the orogenic phases.

Calc-alkaline rocks are represented by massive lava flows including basalts, basaltic andesites, andesites, dacites, and rhyolites, as well as by some granitoid complexes intruded into the ophiolitic sequence. Volcanics show highly porphyritic textures, with clinopyroxene, orthopyroxene, hornblende, and plagioclase phenocrysts, and incompatible-element compositions characterized by Ta-Nb, P, and Ti depletion, as well as by Rb-Ba-Th and La-Ce enrichment. These rocks also show marked light REE enrichments, commonly interpreted to be a consequence of mantle source enrichment by subduction-derived components. Ophiolites represent the remnants of an oceanic basin, whereas calc-alkaline rocks represent a magmatic island-arc setting developed over the previously formed oceanic lithosphere. The geological and petrological data suggest that the South Apuseni

---

[1] Corresponding author; e-mail: marroni@dst.unipi.it

Mountains ophiolites can be correlated with the mid-ocean ridge–type ophiolites of the Vardar zone. They are interpreted to have assumed their present location in the inner zone of the Carpathian belt during the tectonic escape of Adria-related microplates during the Late Paleogene–Early Neogene.

## Introduction

IN THE ALPINE orogenic belts, from the Alps to the Carpathians, orogenic zones are derived from the collision of multiple microplates with the European stable continental plate. The history of these microplates is generally deduced from geophysical and geological data, providing important constraints for their geodynamic reconstruction. In this framework, ophiolites are regarded as a useful tool because they represent remnants of oceanic lithosphere deformed and/or metamorphosed along the main collisional zones.

In the South Apuseni Mountains, located between the North Apuseni Mountains and the Southern Carpathians (western Romania), a magmatic association of Jurassic age has been recognized. This association is characterized by a complex assemblage of Jurassic magmatic series, previously reported as a single ophiolitic sequence (e.g., Radulescu and Sandulescu, 1973; Herz and Savu, 1974). These igneous sequences, as well as the associated sedimentary and metamorphic rocks, are regarded as belonging to the Tisza (also known as Tisia) block, a small continental microplate located behind the Carpathian belt. The objective of this paper is to present a new geological and petrological interpretation of these Jurassic magmatic sequences, in order to provide further constraints for the geodynamic evolution of the Tisza microplate and its relationships with the Carpathian belt.

## Geological Setting of the Apuseni Mountains

The Carpathians are an arcuate orogenic belt of Alpine age. Westward, the Carpathian belt shows a transition to the Eastern Alps, whereas in the southern areas it is linked with the Hellenic-Dinaric belt (Fig. 1). The Carpathian belt originated from Mesozoic–Cenozoic convergence between the subducting European plate and continental fragments derived from the African plate (e.g. Dercourt et al., 1990). The wealth of geophysical and geological data indicates that this convergence resulted in west-dipping subduction of the European lithosphere. The related crustal shortening is well recorded in the complex nappe stack of the Carpathian belt, mainly consisting of basement and cover nappes where the record

of the main Cretaceous–Neogene tectonic events is still recognizable (Ratschbacher et al., 1993; Schmid et al., 1998). Shortening was accomodated by extension in the inner zone of the Carpathian belt, probably connected with an eastward retreat of the European margin (Horvath and Royden, 1981; Royden, 1993; Csontos, 1995; Linzer, 1996). A large sedimentary basin characterized by Neogene deposits and coeval calc-alkaline and alkaline volcanics occurs in this area (Fig. 1). However, this realm, generally indicated in the literature as the Pannonian Basin, is also characterized by outcrops of pre-Neogene metamorphic and magmatic rocks. For instance in the Bükk, Mecsek, Villany, Papuk, and Apuseni mountains, crystalline basement with related Mesozoic sedimentary cover crops out. Moreover, Jurassic magmatic associations have also been found in the Bükk (Aignes-Torres and Koller, 1999) and Apuseni Mountains (Bleahu et al., 1981; Nicolae, 1995).

Geophysical data suggest that these rocks represent the substrate of the Pannonian Basin; the lithotectonic units were derived mainly from an assemblage of different continental microplates, and are generally referred to as the Alcapa, Tisza, and Dacia blocks (Fig. 2). The Alcapa block is located in the northernmost area of the Pannonian Basin, whereas the Tisza and Dacia blocks occur in the southernmost regions. In this paper, the Tisza and Dacia blocks are regarded as microplates with different pre-Tertiary tectonic histories as reflected in paleomagnetic data (Patrascu et al., 1994). The Alcapa block, although regarded as a single microplate, can be subdivided into two different zones: the northern zone can be directly correlated with the Austroalpine units, whereas the southern zone mainly includes tectonic units, referred to as the Southern Alps.

According to geophysical and geological data (Marton et al., 1992), the Alcapa block is separated from the Tisza block by the mid-Hungarian line (Fig. 1), a strike-slip fault probably active since the Cretaceous. The Tisza block is separated from the Southern Carpathians by the south Transylvanian fault (Fig. 1), a first-order tectonic line for which Paleogene–Neogene dextral transpression has been postulated (e.g., Burchfiel, 1980).
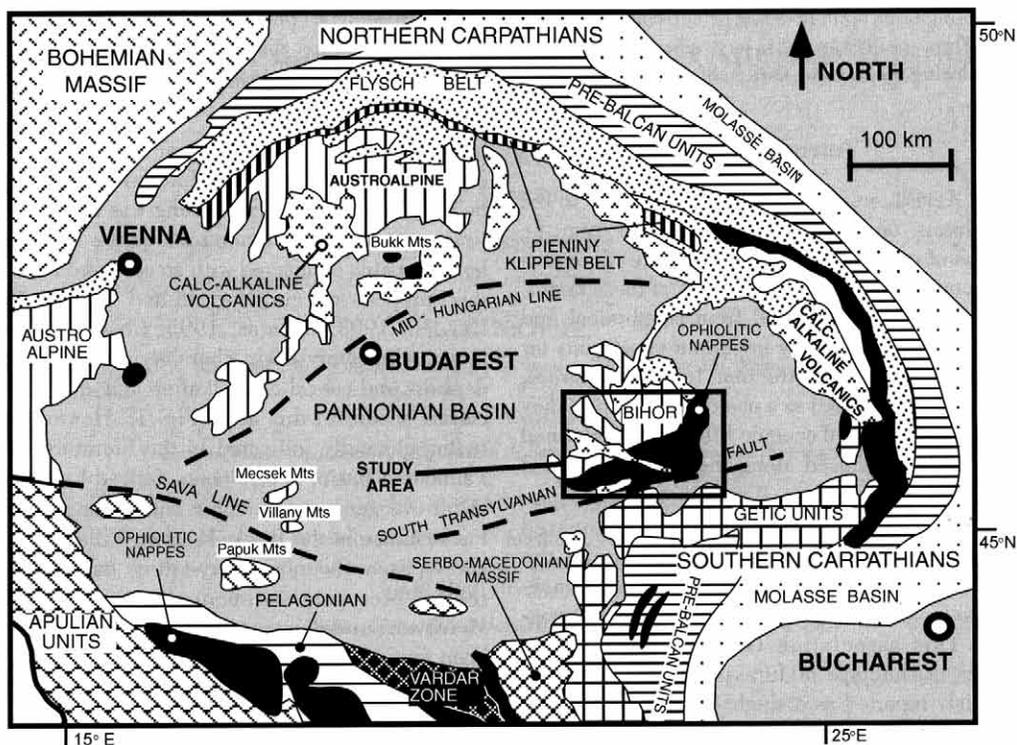
FIG. 1. Distribution of the main geological domains in the Carpathian orogenic area. The box shows the location of the study area.
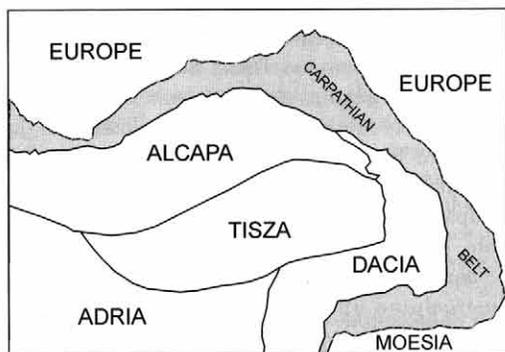


FIG. 2. Main plates of the Carpathian area (after Csontos, 1995)

Geological data suggest that the Alcapa and Tisza blocks were derived from the northernmost edge of the Adria (= Apulia) plate (Sandulescu, 1994). However, the geodynamic evolution of these blocks, regarded as small microplates displaced and rotated during the Neogene, is still matter of debate (e.g., Csontos, 1995; Neugebauer et al., 2001).

The geological setting of the Tisza (also known as the Austro-Bihorean) microplate (Kovacs, 1982; Sandulescu, 1984) includes a stack of continental tectonic units cropping out in the North Apuseni Mountains (Fig. 3). They are represented (from bottom to top), by the Bihor, Codru, and Biharia complexes (Sandulescu, 1984); all consist of polydeformed crystalline basement covered by Permian–Lower Cretaceous sedimentary sequences of Austroalpine affinity. These complexes (also known as the Internal Dacides), were imbricated in two phases with northward to northwestward vergence under low-grade P/T metamorphic conditions during the Cretaceous. As suggested by Ar-Ar radiometric dating (Dallmeyer et al., 1999), the first phase (known as the "Austrian phase") occurred from the Aptian to early Albian, and was marked by sedimentation of Aptian–Albian siliciclastic deposits (indicated in Fig. 3 as Cretaceous flysch units). The relationships between the Bihor, Codru, and Biharia
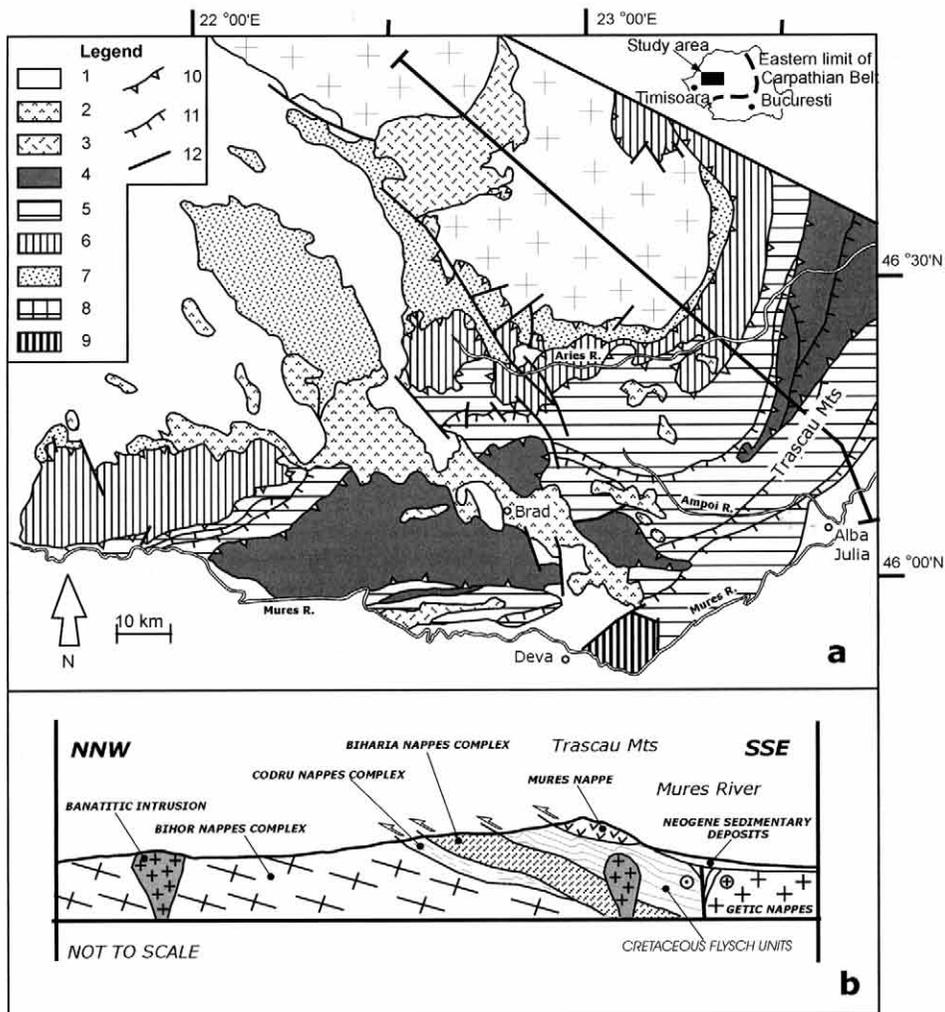
FIG. 3. Tectonic sketch map of the eastern sector of the Apuseni Mountains (A) and schematic cross section across the Trascau Mountains (B); the location of the cross section is indicated in Figure 3A. Legend: 1 = Neogene sedimentary cover; 2 = Neogene calc-alkaline intrusions and related subvolcanic rocks; 3 = Banatitic intrusives and volcanics; 4 = Mures nappe; 5 = Cretaceous flysch units; 6 = Biharia nappes complex; 7 = Codru nappes complex; 8 = Bihor nappes complex; 9 = Getic units; 10 = Main thrusts; 11 = secondary thrusts; 12 = main faults.

complexes after the "Austrian" phase are sealed by Santonian–Campanian "Gosau" deposits.

In the South Apuseni Mountains, the Bihor, Codru, and Biharia complexes as well as the Cretaceous flysch units are overlain by the Mures nappe (Fig. 3), which consists of several tectonic units. This nappe displays the most important ophiolitic sequence of the Carpathian area. According to Bleahu et al. (1981) and Nicolae (1995), the Mures nappe is also characterized by the presence of different igneous units related to distinct tectono-magmatic settings. According to the geological data, the Cretaceous flysch units and the overlying Mures nappe were thrust over the Bihor, Codru, and Biharia complexes during the late Maastrichtian ("Laramian" phase). The subsequent Maastrichtian to Paleocene Banatitic intrusions and related volcanics sealed the relationships between all the tec-

FIG. 4. Relationships between the Middle Jurassic ophiolite sequence, Upper Jurassic calc-alkaline series, Late Jurassic granitoids, and Upper Jurassic–Lower Cretaceous sedimentary deposits.



FIG. 5. Schematic log of the ophiolite sequence from the South Apuseni Mountains.

tonic units of the Apuseni Mountains. Moreover, a Jurassic tectonic event is well recorded by Ar-Ar radiometric datings of the Biharia complex (Dallmeyer et al., 1999): this event is ge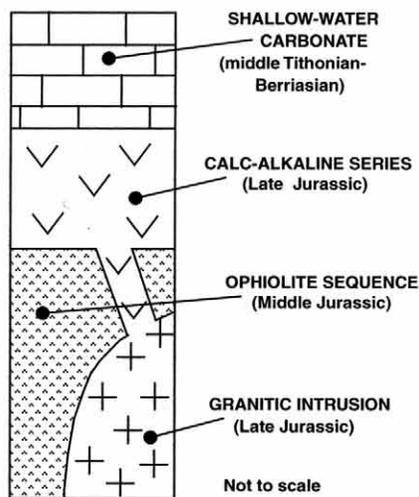nerally considered to be related to closure of the oceanic basin from which the ophiolites of the South Apuseni Mountains were derived.

## The Mures Nappe

### Geology

The South Apuseni Mountains ophiolites (Fig. 4) are strongly dismembered in several tectonic slices (Lupu, 1976; Bleahu et al., 1981; Nicolae, 1995); consequently, a complete sequence cannot be directly observed. However, on the basis of sections observed in the different tectonic slices, a reconstruction of the pseudo-stratigraphical sequence (Fig. 5) can be proposed: this includes a gabbroic intrusive section, followed by a sheeted dike complex showing transition to a volcanic cover. Mantle rocks are absent, and thus these ophiolites represent only the oceanic crustal portion. The intrusive section is represented by small gabbroic bodies showing both layered and isotropic textures, and include scarce ultramafic cumulates, melagabbros, gabbros, and rare gabbronorites associated with ferrogabbros. In the westernmost part of the South Apuseni Mountains, gabbros are overlain by a sheeted dike com-

plex, represented by parallel and subparallel dikes with gabbroic screens. The sheeted dike complex is formed by basaltic and subordinate basaltic-andesitic dikes, from 10 to 50 cm in size. Dike textures include fine-to medium-grained aphyric and plagioclase porphyritic types, with intergranular to doleritic textures and vitrophyric chilled margins. The volcanic sequence includes massive and pillow-lava basalts, with pillow breccias and related arenites occurring between several of the different lava flows. The ophiolitic sequence is capped by few meters of radiolarian cherts (Nicolae et al., 1992).

The entire ophiolite sequence was probably very thick, as suggested by the considerable thickness (> 2 km) of volcanic and subvolcanic rocks. Evidence of ocean-floor metamorphism in both gabbros and basaltic rocks is supported by the occurrences of actinolite and chlorite replacing primary pyroxene, and prehnite ± epidote ± calcite replacing plagioclase. Gabbros are also crosscut by secondary amphibole veinlets.

Ductile deformation and synkinematic metamorphism are absent in the South Apuseni Mountains ophiolites, suggesting that they were dismembered

in multiple slices at shallow structural levels during the orogenic phases. Ophiolites are topped by calc-alkaline magmatic rocks (Bleahu et al., 1981; Nicolae, 1995), including massive lava flows (up to 1000 m thick) ranging from basalts through basaltic andesites, andesites, and dacites to rhyolites. Lava flows up to 20–30m thick are common. Andesitic, dacitic, and rhyolitic calc-alkaline dikes are widespread throughout the ophiolitic sequence.

In the Trascau Mountains (Fig. 3), different ophiolitic units have been recognized (Bleahu et al., 1981; Nicolae, 1995). These mainly comprise an assemblage of ophiolitic basalt slices imbricated with calc-alkaline volcanics and/or slices of Aptian-Albian siliciclastic turbidites.

Some granitoid intrusions with calc-alkaline affinity are located in the southern and western areas of the South Apuseni Mountains (Fig.3), consisting of granites to granodiorites as well as diorites at the margins of the intrusions. Granitic dikes and veins cut both the ophiolitic and calc-alkaline rocks (Bleahu et al., 1981; Nicolae, 1995).

The ages of both ophiolitic and calc-alkaline units are still under debate. Several K/Ar datings on ophiolitic basalts have been performed by Nicolae et al. (1992), and vary greatly from 138.9 ± 6 to 167.8 ± 5 Ma, probably because these age data have been affected by the imprinting of high heat fluxes connected with the intrusion of calc-alkaline dikes. Nonetheless, the oldest age (167.8 ± 5 ma) is in agreement with the Callovian to Oxfordian radiolarian assemblages found in the cherts at the top of the ophiolite sequence (Lupu et al., 1995). This suggests a Middle Jurassic age for the ophiolite sequence. Available K/Ar radiometric datings for the calc-alkaline volcanics are generally unreliable (e.g., Bleahu et al., 1984; Nicolae et al., 1987). Nevertheless, their Late Jurassic age is well constrained by the Oxfordian to lowermost Tithonian microfossils found by Cioflica et al. (1981) in limestones intercalated in the uppermost basalts. The calc-alkaline volcanics are covered by a Middle Tithonian to Berriasian shallow-water carbonate sequence (Lupu, 1983). The available datings for the associated granitoids (155 Ma; Pana, 1998) suggest a short time elapsed between genesis of the ophiolites and that of the overlying calc-alkaline sequence.

## Petrology and Geochemistry

This section is mainly focused on the petrological and geochemical characterization of both ophi-
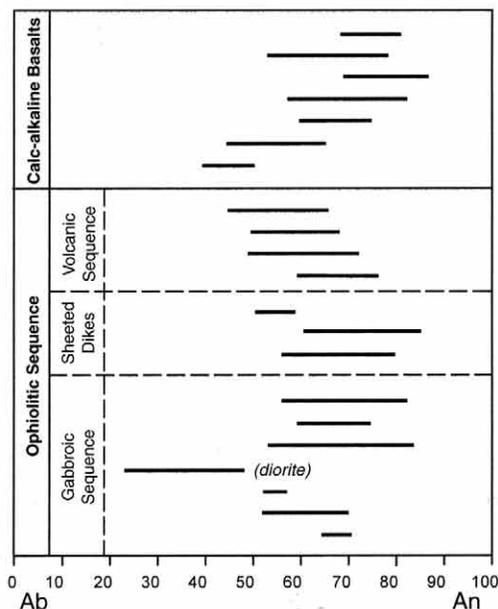


FIG. 6. Composition, expressed in terms of albite and anorthite contents, of plagioclase in the South Apuseni Mountains ophiolitic and calc-alkaline sequences. Bars represent plagioclase compositional range in individual samples.

olitic and calc-alkaline series, and defines their tectono-magmatic environment of formation.

*Analytical techniques*

About 170 rock samples from both ophiolitic and calc-alkaline sequences were analyzed for major oxides and trace elements; from these, 20 representative samples were chosen for REE, Ta, Th, Nb, U, and Sc analyses. Representative analyses are presented in Tables 1 and 2 and illustrated in Figs. 7, 9, 10, 11, and 12. Major and trace elements were determined by X-ray fluorescence (XRF) on pressed powder pellets using a Philips PW-1400 XRF spectrometer and following the full matrix correction method proposed by Franzini (1979). Uncertainty is generally less than 2% for major oxides and less than 5% for trace-element determinations. The detection limits for trace elements range from 1 to 2 ppm. Rare-earth element (REE), Sc, Nb, Hf, Ta, Th, and U analyses were performed by inductively coupled plasma–mass spectrometry (ICP-MS) using a VG Elemental Plasma Quad PQ2 Plus. Plus/minus error, calculated by analyzing several international standards, varies from 1 to 8%. Detection limits are
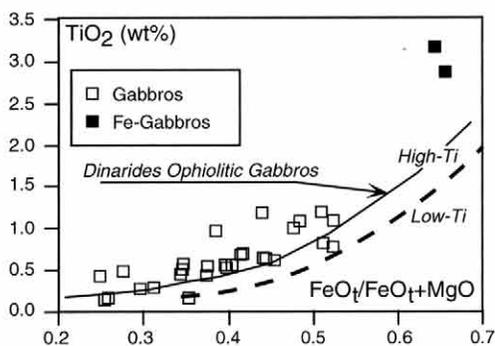
FIG. 7. FeO/MgO versus TiO$_2$ discrimination diagram for the South Apuseni Mountains ophiolitic gabbros, modified after Serri (1981). The dashed line separates the fields for high-Ti and low-Ti ophiolites. The solid line indicates the fractionation trend of gabbroic rocks from the Dinarides ophiolites (Ivanov et al., 1987; Lugovich et al., 1991; Trubelja et al., 1995).

(in ppm): Sc = 0.29; Nb, Hf, Ta = 0.02; REE <0.14; Th, U = 0.011. Both XRF and ICP-MS analyses were performed at the University of Ferrara, Italy.

Electron microprobe mineral analyses were performed using a JEOL-JXA 8600 automated microanalyzer at the University of Florence. The operative conditions were: sample current of 10nA and accelerating potential of 15KV. Counting time was 100 seconds per peak and 20 sec for background positions. Results are presented in Figures 6 and 8.

### Ophiolitic sequence

The ultramafic cumulates, although uncommon, exhibit a wide range of compositions, including olivine-websterites, plagioclase-dunites, and plagioclase-wehrlites. Although these rocks are strongly altered, the cumulate textures are commonly preserved and are characterized by olivine (± plagioclase) as cumulus phases, and poikilitic pyroxene as intercumulus minerals suggesting the following crystallization order: (Cr-spinel) + olivine – plagioclase, clinopyroxene – orthopyroxene, that is, a typical MORB crystallization trend.

The ultramafic cumulates show a transition to gabbros, in turn represented by small plutonic bodies including olivine-gabbros, gabbros, leucogabbros, Fe-gabbros, and quartz-diorites, as well as rare gabbronorites. Texturally, gabbroic rocks can be subdivided into cumulitic and isotropic types, both characterized by a plagioclase – clinopyroxene –

orthopyroxene crystallization order. Plagioclase is commonly affected by ocean-floor hydrothermal alteration; however, fresh crystals display a wide range of compositions, as summarized in Figure 6. Clinopyroxene is commonly poikilitic in cumulitic gabbros, and anhedral to interstitial in isotropic gabbros, compositionally ranging from diopside to augite and rarely extending to endiopside.

On the basis of their geochemical compositions (in particular with regard to TiO$_2$ content and FeO/FeO+MgO ratio), gabbros show a clear high-Ti magmatic affinity (Fig. 7). TiO$_2$ content in gabbros ranges from 0.43 wt% to 2.58 wt%, while in Fe-gabbros it is included between 2.85 wt% and 3.12 wt%. The overall geochemical characteristics (Table 1) display a wide range of variation, reflecting the cumulitic versus isotropic nature of these gabbros, as well as their wide degrees of fractionation (Mg# = 85–64 in gabbros and 53–51 in Fe-gabbros).

The sheeted dike complex is formed by basaltic and subordinate basaltic-andesitic dikes. The general chemical compositions of mineralogical phases compare closely with those of MORB, as exemplified by clinopyroxene compositions plotted in the discrimination diagrams of Figure 8. As shown in Figure 6, fresh plagioclase displays a wide range of compositions; indeed, chemical variations between different crystals within each sample and from core to rim of individual crystals are considerable. These chemical variations reflect a continuous supply of primitive melts in the magma chamber in a mid-ocean ridge setting. Although sheeted dikes display a geochemical composition slightly different from the overlying basalts (Table 1), they share the same magmatic affinity with these. Actually, the dikes are characterized by high contents of the less mobile elements such as: TiO$_2$ (1.25–3.24 wt%), P$_2$O$_5$ (0.23–0.41 wt%), Y (38–75 ppm) and Zr (102–287 ppm). Mg# (60.8–46), Cr (33–370 ppm), and Ni (20–92 ppm), suggesting that these magmas are moderately differentiated. A clear high-Ti magmatic affinity is indicated in the Ti/V discrimination diagram (Fig. 9), as well as in incompatible-element concentrations shown in Figure 10A. Figure 9 also shows the highest degree of fractionation of sheeted dike basalts with respect to the volcanic basalts.

The volcanic sequence, which is predominantly composed of basalts and minor basaltic andesites, is by far the most abundant portion in the ophiolitic sequence. Basalts mainly occur as massive and pillow lava flows, although minor basaltic breccias occur in many localities. Textures are commonly

TABLE 1. Representative Major- and Trace-Element Compositions for the Jurassic Ophiolitic Rocks from the South Apuseni Mountains[1]

| Sample: | Gabbros | | | Sheeted dikes and volcanic sequence | | | | | Dikes | | |
|---|---|---|---|---|---|---|---|---|---|---|---|
| | AP126 | AP177 | AP179 | AP123C | AP123A | AP136 | AP 24 | AP104 | AP118 | AP151 | AP147 |
| Rock: | Gb | Gb | Fe-Gb | Bas | Bas | Bas | Bas | Bas | Bas | Bas | Bas |
| Note: | | | | Sh-Di | Sh-Di | MLF | Pillow | Pillow | in Bas | in Bas | in Gb |
| XRF analyses | | | | | | | | | | | |
| $SiO_2$ | 56.17 | 48.26 | 41.67 | 48.11 | 51.55 | 47.64 | 47.11 | 45.23 | 45.88 | 47.84 | 55.48 |
| $TiO_2$ | 1.17 | 1.07 | 3.12 | 1.25 | 2.52 | 1.82 | 1.00 | 0.80 | 0.99 | 1.25 | 1.45 |
| $Al_2O_3$ | 16.89 | 15.13 | 15.06 | 17.84 | 12.36 | 15.72 | 13.79 | 14.10 | 15.72 | 14.80 | 16.19 |
| $Fe_2O_3$ | 0.67 | 1.27 | 2.04 | 1.33 | 1.72 | 1.55 | 1.19 | 0.98 | 1.29 | 0.84 | 0.87 |
| FeO | 4.45 | 8.50 | 13.63 | 8.88 | 11.48 | 10.34 | 7.95 | 6.54 | 8.62 | 5.58 | 5.80 |
| MnO | 0.07 | 0.14 | 0.20 | 0.16 | 0.16 | 0.19 | 0.15 | 0.13 | 0.14 | 0.09 | 0.09 |
| MgO | 4.88 | 10.24 | 8.65 | 7.33 | 5.77 | 7.61 | 10.18 | 10.43 | 10.55 | 4.52 | 5.19 |
| CaO | 8.97 | 11.62 | 12.80 | 11.03 | 8.34 | 10.24 | 9.44 | 12.47 | 7.20 | 13.36 | 7.41 |
| $Na_2O$ | 4.14 | 1.62 | 1.76 | 2.39 | 4.47 | 2.63 | 3.45 | 2.89 | 3.38 | 5.19 | 4.24 |
| $K_2O$ | 0.26 | 0.06 | 0.13 | 0.25 | 0.21 | 0.29 | 0.16 | 0.31 | 0.51 | 0.79 | 0.07 |
| $P_2O_5$ | 0.56 | 0.09 | 0.09 | 0.24 | 0.34 | 0.29 | 0.12 | 0.16 | 0.15 | 0.20 | 0.27 |
| LOI | 1.78 | 2.01 | 0.85 | 1.19 | 1.08 | 1.68 | 5.46 | 5.95 | 5.57 | 5.53 | 2.94 |
| Total | 100.00 | 100.00 | 100.00 | 100.00 | 100.00 | 100.00 | 100.00 | 100.00 | 100.00 | 100.00 | 100.00 |
| Mg# | 66.16 | 68.22 | 53.08 | 59.55 | 47.26 | 56.74 | 69.5 | 73.96 | 68.58 | 59.09 | 61.47 |
| Ba | 43 | 55 | 20 | 38 | 41 | 44 | 52 | 34 | 37 | 146 | 48 |
| Rb | < 2 | n.d. | 3 | 2 | n.d. | 3 | 3 | 7 | 11 | 18 | n.d. |
| Sr | 201 | 190 | 220 | 129 | 164 | 170 | 172 | 180 | 104 | 312 | 267 |
| Th | 4 | n.d. | n.d. | | | | | | | | < 2 |
| Zr | 72 | 32 | 20 | 102 | 191 | 137 | 69 | 57 | 69 | 85 | 118 |
| Nb | 9 | 3 | < 2 | | | | | | | | 4 |
| Y | 51 | 21 | 16 | 38 | 55 | 44 | 32 | 21 | 27 | 27 | 36 |
| V | 187 | 393 | 980 | 256 | 487 | 347 | 287 | 216 | 279 | 220 | 290 |
| Cr | 72 | 126 | 63 | 371 | 45 | 270 | 129 | 674 | 40 | 275 | 15 |
| Ni | 38 | 63 | 13 | 92 | 25 | 79 | 55 | 371 | 37 | 66 | 13 |
| Co | 18 | 46 | 58 | 40 | 37 | 43 | 40 | 51 | 42 | 21 | 32 |
| Pb | 3 | 3 | n.d. | 3 | n.d. | n.d. | 6 | 4 | 7 | 6 | n.d. |
| Zn | 23 | 30 | 83 | 87 | 41 | 109 | 46 | 67 | 81 | 67 | 16 |
| La | 15 | 3 | 3 | | | | | | | | 11 |
| Ce | 46 | n.d. | 12 | | | | | | | | 31 |
| ICP-MS analyses | | | | | | | | | | | |
| Ta | | | | 0.23 | 0.62 | 0.35 | 0.37 | 0.17 | 0.13 | 0.36 | |
| Th | | | | 0.16 | 0.66 | 0.25 | 0.16 | 0.44 | 0.36 | 0.32 | |
| Nb | | | | 2.71 | 6.94 | 4.03 | 1.25 | 1.73 | 1.48 | 1.33 | |
| Hf | | | | 2.72 | 3.80 | 3.39 | 1.01 | 1.12 | 1.51 | 2.09 | |
| U | | | | 0.06 | 0.19 | 0.09 | 0.04 | 0.33 | 0.09 | 0.33 | |
| Sc | | | | 99.1 | 93.5 | 105 | 150 | 121 | 104 | 76.5 | |
| La | | | | 3.78 | 8.94 | 5.41 | 2.05 | 3.09 | 3.49 | 3.17 | |
| Ce | | | | 12.1 | 25.9 | 17.0 | 6.14 | 8.05 | 9.78 | 10.8 | |
| Pr | | | | 1.99 | 4.10 | 2.75 | 1.09 | 1.25 | 1.62 | 1.59 | |
| Nd | | | | 10.8 | 21.6 | 14.9 | 6.14 | 6.26 | 8.66 | 8.39 | |
| Sm | | | | 3.81 | 6.84 | 4.94 | 2.12 | 1.79 | 2.69 | 2.69 | |
| Eu | | | | 1.37 | 2.23 | 1.73 | 0.76 | 0.61 | 0.98 | 0.97 | |
| Gd | | | | 4.59 | 8.40 | 6.24 | 2.69 | 2.14 | 3.33 | 3.09 | |
| Tb | | | | 0.92 | 1.61 | 1.20 | 0.53 | 0.40 | 0.63 | 0.57 | |
| Dy | | | | 5.98 | 10.7 | 7.69 | 3.49 | 2.55 | 3.94 | 3.72 | |
| Ho | | | | 1.27 | 2.22 | 1.61 | 0.75 | 0.54 | 0.84 | 0.75 | |
| Er | | | | 3.80 | 6.51 | 4.77 | 2.18 | 1.60 | 2.43 | 2.19 | |
| Tm | | | | 0.50 | 0.88 | 0.64 | 0.32 | 0.23 | 0.35 | 0.28 | |
| Yb | | | | 3.53 | 5.92 | 4.41 | 2.16 | 1.63 | 2.29 | 1.99 | |
| Lu | | | | 0.52 | 0.83 | 0.65 | 0.30 | 0.23 | 0.32 | 0.28 | |

[1]Abbreviations- Gb: gabbro, Fe-Gb: ferrogabbro, Bas: basalt, BA: basaltic andesite, Sh-Dy: sheeted dike complex, MLF = massive lava flow; n.d. = not detected.
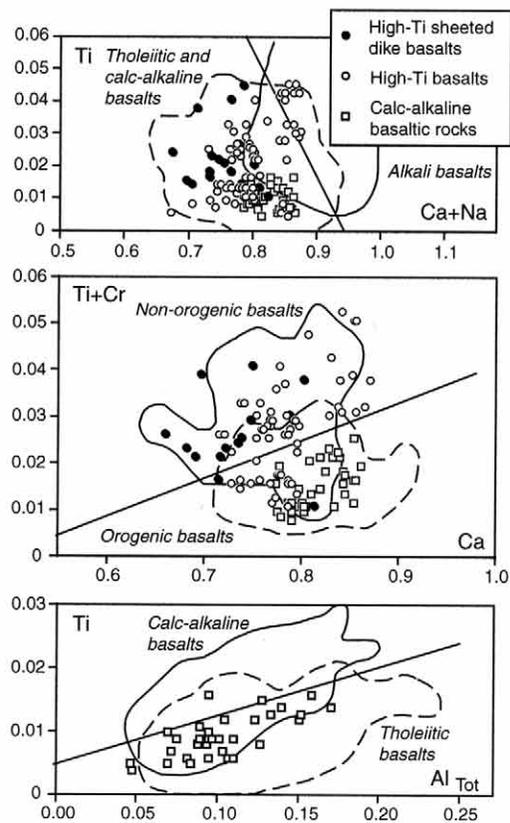
FIG. 8. Clinopyroxene discrimination diagrams for South Apuseni Mountains ophiolitic basalts and calc-alkaline volcanics, modified after Leterrier et al. (1982).
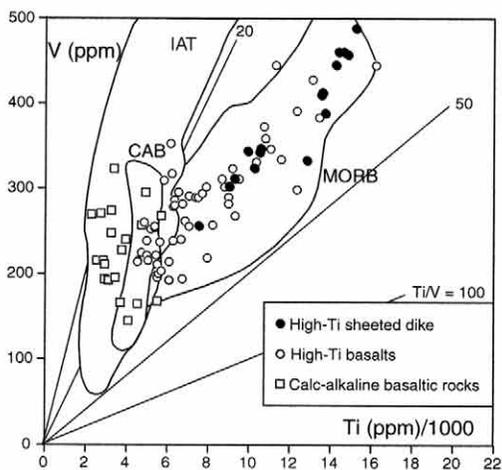


FIG. 9. Ti/1000 versus V discrimination diagram for South Apuseni Mountains mafic volcanic rocks. Modified after Shervais (1982). Abbreviations: IAT = island-arc tholeiites; CAB = calc-alkaline basalts; MORB = mid-ocean ridge basalts.

aphyric to moderately porphyritic, with intersertal, intergranular, and ophitic to sub-ophitic groundmass. All samples from the volcanic sequence are hydrothermally metamorphosed, with plagioclase partially replaced by albite. However, fresh plagioclase ranges from $An_{55}$ to $An_{85}$ (Fig. 6). Clinopyroxene has frequently been replaced by actinolite-hornblende, although fresh samples plot in the field for MORB compositions in the discrimination diagram of Figure 8. Basaltic rocks show a wide range of geochemical compositions (Table 1), as well as fractionation extent (Mg# = 70–40). Compared with the sheeted dike rocks, lavas show lower contents in high-field-strength elements (HFSE). Nevertheless, their high-Ti (MORB) geochemical affinity is clearly indicated by the $TiO_2$ content (0.73–2.98 wt%), $P_2O_5$ (0.13–0.42 wt%), Y (20–68 ppm) and Ti/V

ratios (20–40; Fig. 9). Moreover, FeO and $TiO_2$ increase during fractionation, and the N-MORB–normalized incompatible-element patterns (Fig. 10A) are consistent with the compositions of present-day MORB. The considerable enrichment in low-field-strength elements (LFSE) may be related to the high degree of alteration generally experienced by the studied samples. Chondrite-normalized REE patterns (Fig.11A) are rather flat or slightly enriched in light REE (LREE) with respect to medium and heavy REE (HREE). In general, $(La/Sm)_N$ ratios vary from 0.75 to 1.11, whereas $(La/Yb)_N$ ratios are included between 0.85 and 1.69. Only the most primitive analyzed sample (AP24) displays LREE depletion relative to medium and HREE, with $(La/Sm)_N = 0.62$, $(La/Yb)_N = 0.68$, and $(Sm/Yb)_N = 1.09$. REE abundances reflect typical MORB composition, as well as various degrees of fractionation, ranging from ~10 to 50 × chondritic abundance. The Eu negative anomalies observed in the more evolved samples (Fig. 11A) reflect previous removal of early crystallized plagioclase. The perfect similarity between sheeted dikes and the volcanic sequence (Fig. 11A) indicate their co-genetic origin. In summary, all the data presented in this paper suggest that the ophiolites of the South Apuseni Mountains were generated in a mid-ocean ridge setting.
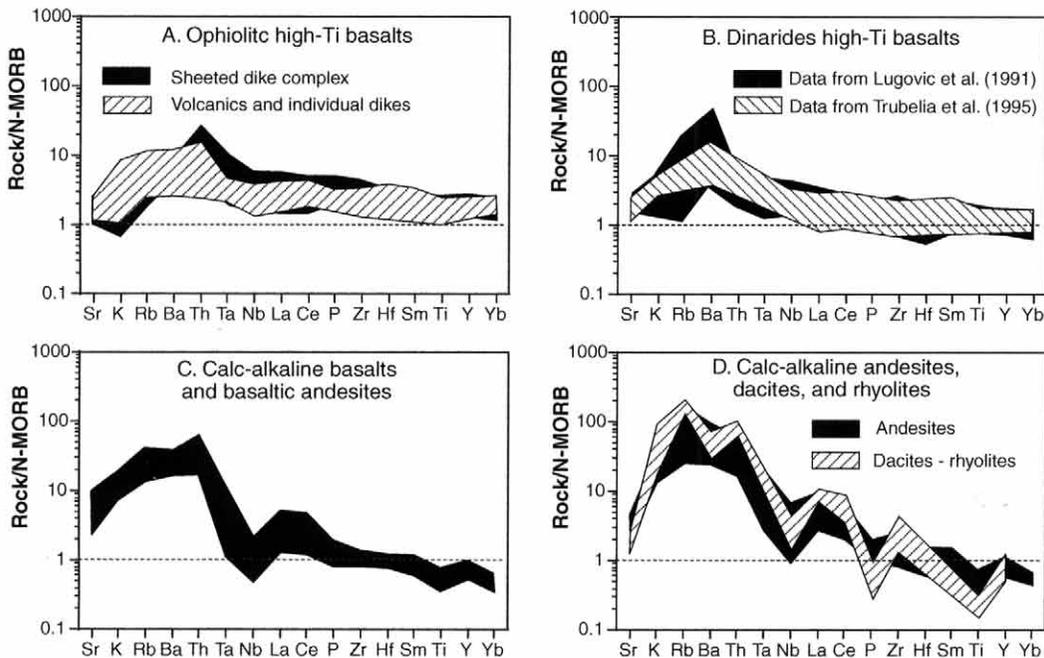
FIG. 10. N-MORB–normalized incompatible-element diagrams for Jurassic magmatic associations of the South Apuseni Mountains. Normalizing values are from Sun and McDonough (1989). A. South Apuseni Mountains high-Ti ophiolitic basalts. B. Dinarides Vardar Zone high-Ti basalts. C. South Apuseni Mountains calc-alkaline basalts and basaltic andesites. D. Calc-alkaline andesites, dacites, and rhyolites.

## Calc-alkaline series

Calc-alkaline volcanic and subvolcanic rocks range from basalts, basaltic andesites, andesites, and dacites to rhyolites. However, while basaltic andesites are the most represented rock type in the volcanic sequence, dikes are largely dominated by andesites, dacites, and rhyolites. Representative chemical analyses of island-arc volcanic and subvolcanic rocks of the South Apuseni Mountains are presented in Table 2. According to the classification diagram shown in Figure 12 (Miyashiro, 1974), both volcanic and subvolcanic rocks exhibit a clear calc-alkaline affinity. All volcanic rock types characteristically show highly porphyritic textures, where the phenocryst assemblage is dominated by clinopyroxene, orthopyroxene and plagioclase. Mg-hornblende is locally found in basaltic andesites, andesites, and rhyolites. From Figure 6 it can be observed that plagioclase phenocrysts vary greatly in composition in basalts and basaltic andesites ($An_{45}$-$An_{85}$), whereas An contents decrease in rhyolites ($An_{40}$-$An_{50}$). Clinopyroxene phenocrysts from the calc-alkaline series are substantially subalkaline (Fig.8), and are

similar to those of the calc-alkaline basalts described by Leterrier et al. (1982). Titanomagnetite and magnetite are common Fe-Ti oxide phases.

Calc-alkaline basalts can be clearly distinguished from MORBs in the Ti/1000 versus V diagram of Figure 9, where calc-alkaline basalts plot in the compositional field for calc-alkaline and island-arc rocks proposed by Shervais (1982). N-MORB–normalized incompatible-element patterns for calc-alkaline basalts and basaltic andesites (Fig. 10C) show the typical patterns of oceanic calc-alkaline basaltic rocks (Pearce, 1983) characterized by Ta-Nb and Ti negative anomalies, as well as Rb-Ba-Th and La-Ce spikes. The magnitude of both positive and negative anomalies increases in andesites, dacites, and rhyolites, where significant negative P and positive Rb anomalies can also be observed (Fig. 10D). In general, calc-alkaline rocks show decreasing abundances of HFSE, such as P, Ti, and Y, with increasing $SiO_2$. Negative Nb anomalies are observed in modern arc volcanics, and are thought to reflect formation in a supra-subduction zone (Briqueu et al., 1984). In addition, the enrichment of
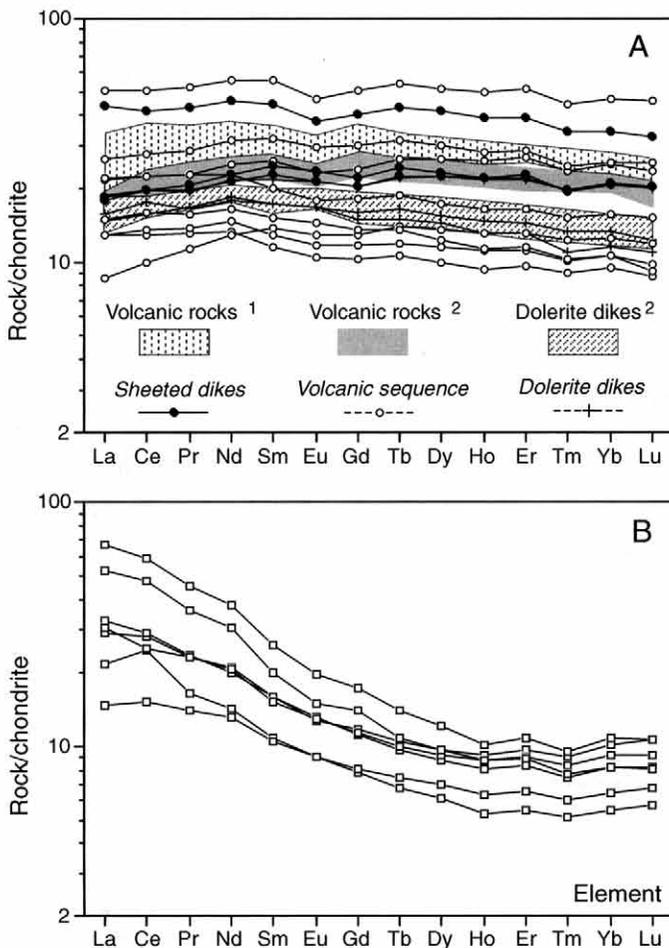
FIG. 11. Chondrite-normalized REE patterns for Jurassic magmatic associations of the South Apuseni Mountains. Normalizing values after Sun and McDonough (1989). A. Ophiolitic high-Ti basalts and basaltic andesites. B. Calc-alkaline basalts and basaltic andesites.

LFSE relative to HFSE is attributed to the enrichment of the mantle wedge by LILE-enriched fluids derived from the subducted oceanic crust.

The calc-alkaline differentiation trend also is indicated by the $Al_2O_3$-FeO-MgO (AFM) relative content variations (Table 2), which reflect suppression of FeO enrichment due to crystallization of Fe-Ti oxides in the early stages of magmatic evolution. Calc-alkaline basalts and basaltic andesites exhibit marked LREE enrichments with respect to HREE (Fig. 11B), commonly interpreted as a consequence of mantle source enrichment by subduction-derived components. Such enrichment is exemplified by the $(La/Yb)_N$ ratios, which range from 2.3 to 6.3.

## Comparison with Ophiolites from the Alpine-Apennine and Dinaric–Hellenic Belts

According to Dercourt et al. (1990), the South Apuseni Mountains ophiolites represent an oceanic basin that originated during the Middle Jurassic in an area of complex plate geometry. In this area, several amalgamated continental blocks located at the northernmost edge of the Adria plate were separated from the European plate by small oceanic domains. These domains are attributed to the two main oceanic branches of the Tethys (i.e., the Ligure-Piemontese and Vardar oceanic basins), which were very

TABLE 2. Representative Major- and Trace-Element Compositions for Jurassic Calc-Alkaline Rocks from the South Apuseni Mountains[1]

| | Volcanic sequence | | | | | | | | | Dikes | |
|---|---|---|---|---|---|---|---|---|---|---|---|
| Sample: | 597 | AP 22 | AP95A | AP 37 | AP157 | AP 91 | V-3 | AP156 | V/H | AP 32 | AP 33 |
| Rock: | Bas | Bas | Bas | BA | BA | BA | A | A | Rhy | A | D |
| Note: | MLF | MLF | MLF | MLF | MLF | MLF | MLF | MLF | MLF | in HT-B | in HT-B |
| | | | | | *XRF analyses* | | | | | | |
| $SiO_2$ | 48.81 | 44.85 | 48.67 | 51.48 | 56.12 | 54.45 | 55.15 | 54.68 | 70.58 | 52.38 | 60.75 |
| $TiO_2$ | 0.89 | 0.60 | 0.89 | 0.55 | 0.51 | 0.47 | 0.57 | 0.46 | 0.33 | 0.72 | 0.39 |
| $Al_2O_3$ | 17.47 | 16.17 | 19.68 | 14.94 | 19.13 | 17.40 | 16.09 | 16.96 | 15.30 | 15.73 | 18.10 |
| $Fe_2O_3$ | 0.96 | 0.99 | 0.91 | 0.79 | 0.84 | 0.89 | 0.75 | 0.60 | 0.27 | 0.85 | 0.51 |
| FeO | 6.41 | 6.61 | 6.09 | 5.27 | 5.63 | 5.92 | 5.02 | 3.98 | 1.80 | 5.63 | 3.43 |
| MnO | 0.15 | 0.12 | 0.12 | 0.09 | 0.12 | 0.09 | 0.11 | 0.26 | 0.07 | 0.11 | 0.07 |
| MgO | 7.58 | 14.05 | 7.66 | 3.96 | 3.82 | 5.13 | 5.30 | 2.90 | 0.51 | 7.73 | 2.04 |
| CaO | 6.52 | 5.74 | 9.24 | 13.68 | 7.84 | 7.34 | 7.37 | 12.35 | 1.74 | 5.82 | 4.82 |
| $Na_2O$ | 3.93 | 1.01 | 2.82 | 2.73 | 3.20 | 2.82 | 2.82 | 2.45 | 3.10 | 4.02 | 3.90 |
| $K_2O$ | 0.67 | 0.68 | 1.23 | 1.35 | 0.54 | 0.96 | 1.36 | 0.66 | 5.31 | 1.33 | 2.20 |
| $P_2O_5$ | 0.21 | 0.08 | 0.11 | 0.19 | 0.14 | 0.11 | 0.16 | 0.15 | 0.08 | 0.14 | 0.14 |
| LOI | 6.40 | 9.08 | 2.57 | 4.96 | 2.12 | 4.43 | 5.28 | 4.56 | 0.93 | 5.55 | 3.64 |
| Total | 100.00 | 100.00 | 100.00 | 100.00 | 100.00 | 100.00 | 100.00 | 100.00 | 100.00 | 100.00 | 100.00 |
| | | | | | | | | | | | |
| mg# | 67.8 | 79.1 | 69.15 | 57.2 | 54.77 | 60.7 | 65.3 | 56.47 | 33.4 | 71.0 | 51.5 |
| | | | | | | | | | | | |
| Ba | 195 | 141 | 249 | 247 | 107 | 119 | 215 | 123 | 471 | 406 | 277 |
| Rb | 23 | 19 | 27 | 19 | 8 | 12 | 27 | 9 | 101 | 33 | 76 |
| Sr | 884 | 217 | 334 | 458 | 330 | 419 | 404 | 283 | 201 | 358 | 480 |
| Th | 8 | | n.d. | | | | | | 11 | 5 | 8 |
| Zr | 101 | 70 | 62 | 89 | 86 | 85 | 144 | 60 | 154 | 134 | 167 |
| Nb | 5 | | n.d. | | | | | | 5 | 5 | 9 |
| Y | 27 | 16 | 23 | 16 | 21 | 16 | 24 | 15 | 18 | 25 | 22 |
| V | 268 | 241 | 168 | 196 | 193 | 212 | 142 | 195 | 40 | 166 | 64 |
| Cr | 69 | 550 | 303 | 265 | 26 | 43 | 154 | 38 | 7 | 161 | 8 |
| Ni | 45 | 223 | 89 | 61 | 15 | 18 | 62 | 26 | 2 | 56 | 3 |
| Co | 28 | 38 | 31 | 24 | 17 | 22 | 22 | 20 | 2 | 26 | 9 |
| Pb | 13 | 20 | 4 | 10 | 10 | 7 | 12 | 8 | 12 | 10 | 13 |
| Zn | 99 | 97 | 55 | 44 | 67 | 71 | 59 | 57 | 30 | 78 | 51 |
| La | 13 | n.d. | | | | | | | 25 | 16 | 19 |
| Ce | 35 | n.d. | | | | | | | 44 | 33 | 42 |
| | | | | | | | | | | | |
| | | | | | *ICP-MS analyses* | | | | | | |
| Ta | | 0.15 | | 0.42 | 0.20 | 0.19 | 0.35 | 0.17 | | | |
| Th | | 2.25 | | 5.14 | 2.45 | 2.96 | 5.90 | 2.31 | | | |
| Nb | | 1.11 | | 4.18 | 2.34 | 1.78 | 3.78 | 1.44 | | | |
| Hf | | 1.62 | | 2.58 | 2.36 | 2.22 | 3.31 | 1.61 | | | |
| U | | 0.60 | | 1.58 | 0.64 | 0.74 | 1.92 | 1.21 | | | |
| Sc | | 59.9 | | 53.6 | 59.8 | 61.1 | 61.4 | 80.3 | | | |
| La | | 3.47 | | 12.4 | 7.0 | 7.3 | 15.9 | 7.7 | | | |
| Ce | | 9.41 | | 29.3 | 17.2 | 15.6 | 35.9 | 17.8 | | | |
| Pr | | 1.33 | | 3.43 | 2.20 | 2.20 | 4.32 | 2.24 | | | |
| Nd | | 6.20 | | 14.3 | 9.81 | 9.74 | 17.7 | 9.39 | | | |
| Sm | | 1.62 | | 3.06 | 2.44 | 2.34 | 3.97 | 2.44 | | | |
| Eu | | 0.53 | | 0.87 | 0.74 | 0.75 | 1.15 | 0.77 | | | |
| Gd | | 1.66 | | 2.90 | 2.42 | 2.35 | 3.60 | 2.30 | | | |
| Tb | | 0.28 | | 0.41 | 0.39 | 0.37 | 0.53 | 0.36 | | | |
| Dy | | 1.76 | | 2.47 | 2.47 | 2.36 | 3.07 | 2.22 | | | |
| Ho | | 0.36 | | 0.50 | 0.52 | 0.49 | 0.58 | 0.45 | | | |
| Er | | 1.09 | | 1.48 | 1.60 | 1.51 | 1.78 | 1.38 | | | |
| Tm | | 0.16 | | 0.19 | 0.23 | 0.21 | 0.24 | 0.19 | | | |
| Yb | | 1.10 | | 1.41 | 1.71 | 1.56 | 1.83 | 1.39 | | | |
| Lu | | 0.17 | | 0.21 | 0.27 | 0.23 | 0.27 | 0.21 | | | |

[1]Abbreviations: Bas = basalt; BA = basaltic andesite; A = andesite; D = dacite, Rhy = rhyolite, MLF = massive lava flow, HT-B = high-Ti ophiolitic basalts; n.d. = not detected.

close to each other at the northernmost edge of the Adria plate. Owing to the complex Cretaceous–Tertiary geodynamic evolution of the Carpathian area, the original location of these ophiolite sequences in the Ligure-Piemontese or Vardar oceanic basins is still a matter of debate.

Previously outlined geological and petrological characteristics can provide useful constraints for determining the original paleogeographic location of the South Apuseni Mountains ophiolites. Several lines of evidence suggest a strict correlation with the Hellenic-Dinaric belt ophiolites, as suggested also by Sandulescu (1994) and Zacher and Lupu (1998).

Characteristics of the South Apuseni Mountains ophiolites (e.g., the presence of a well-developed sheeted dike complex and the relevant thickness of the basalts), can be compared with those of the Hellenic-Dinaric belt ophiolites (e.g., Lugovich et al., 1991 and quoted references). The lack of penetrative deformation and very thin radiolarian cherts as the sole ophiolitic sedimentary cover further characterized the MORB ophiolites of the Hellenic-Dinaric belt. This correlation is also supported by the occurrence of Callovian to Oxfordian radiolarites, similar in age to those from the Guevgueli ophiolites (Danelian et al., 1996), which represent the best-preserved ophiolite sequence from the Vardar oceanic basin. These radiolarites are older than the deposits generally found at the top of the Ligure-Piemontese ophiolites (e.g., Abbate et al., 1986). Moreover, the occurrence of Middle Tithonian to Berriasian shallow-water carbonate deposits (Lupu, 1983) at the top of the sequence is typical of the Hellenic-Dinaric ophiolites. These shallow-water carbonates are interpreted as deposits postdating obduction of the ophiolites (e.g., Robertson, 1994), suggesting that the South Apuseni Mountains ophiolites were already emplaced during the Late Jurassic, as also reognized in the ophiolites of the Hellenic-Dinaric belt. By contrast, the Ligure-Piemontese ophiolites never display any indications of convergence-related events of Late Jurassic age (Abbate et al., 1980).

The most striking evidence for this correlation is provided by the close association of South Apuseni Mountains ophiolites with subduction-related magmatic associations, i.e., the Upper Jurassic island-arc volcanics and related granitoid intrusions. This setting strongly resembles that of the of the Fanos area (Bebien et al., 1987), where MORB rocks are intruded by Late Jurassic calc-alkaline granites.
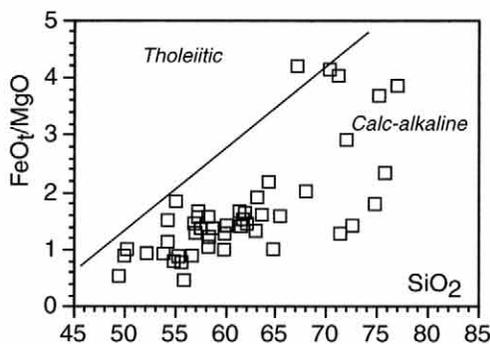


FIG. 12. $SiO_2$ (wt%) versus FeOt/MgO discrimination diagram for the South Apuseni Mountains island-arc volcanic rocks, modified after Miyashiro (1974).

Several geochemical analogies between the South Apuseni Mountains and Hellenic-Dinaric belt ophiolites can also be observed. The average distributional trend of gabbroic rocks from the Hellenic-Dinaric belt ophiolites (Ivanov et al., 1987; Lugovich et al., 1991; Trubelja et al., 1995) is plotted together with gabbros from the South Apuseni Mountains ophiolites (Fig. 7), where close similarities can be seen. Similarly, close compositional analogies, expressed in terms of incompatible-element abundances, between the South Apuseni Mountains and Hellenic-Dinaric ophiolitic basalts can be detected (Lugovich et al., 1991; Trubelja et al., 1995) (Figs. 10A and 10B). However, the most convincing evidence of strict geochemical similarities between the two ophiolitic series is provided by the REE contents displayed by both subvolcanic and volcanic basaltic rocks (Fig. 11A). In fact, most high-Ti basalts from the South Apuseni Mountains ophiolites, although showing various degrees of fractionation, are characterized by essentially flat chondrite-normalized REE patterns. The $(La/Yb)_N$ ratios can be used to summarize the LREE/HREE relative enrichments. In high-Ti basalts from the South Apuseni Mountains, this ratio varies (with the exception of a rather primitive basalt) from 0.85 to 1.69, with an average value of 1.19. Although some LREE-depleted basalts are present, similarly flat REE patterns (Fig. 11A) are displayed by most of the high-Ti basalts from the Hellenic-Dinaric ophiolites (Lugovich et al., 1991; Trubelja et al., 1995), which are characterized by $(La/Yb)_N$ ratios averaging 1.12 (Lugovich et al., 1991) and 0.96 (Trubelja et al., 1995).

In contrast, high-Ti basaltic rocks from the Eastern Alps, Northern Apennine Internal Ligurides, and Albania are characterized by relative depletion of LREE with respect to HREE. The $(La/Yb)_N$ ratios displayed by the Eastern Alps (Venturelli et al, 1981) and Albanian (our unpublished data) ophiolitic basalts are always lower than 0.81 and 0.88, respectively. Although characterized by fairly variable $(La/Yb)_N$ ratios, basalts from the Northern Apennine Internal Ligurides (Venturelli et al., 1981; Ottonello et al., 1984) and Corsica (Venturelli et al., 1981) display ratios that are generally lower than those observed in the Hellenic-Dinaric belt and South Apuseni Mountains ophiolites.

In summary, the geological and geochemical data suggest a strict correlation of the South Apuseni Mountains ophiolites with those of the Hellenic-Dinaric belt. According to Pamic (1983), ophiolites from the Hellenic-Dinaric belt can be subdivided into two different types: the eastern type is characterized by a harzburgitic mantle coupled with IAT basalts, whereas the western one is distinguished by a lherzolitic mantle associated with MOR basalts. The South Apuseni ophiolites can thus be directly correlated with the western type ophiolites characterizing the northernmost edge of the Hellenic-Dinaric belt (Fig.1).

## Geodynamic Implications

The correlation of the South Apuseni Mountains ophiolites with those from the Hellenic-Dinaric belt provides some valuable constraints for reconstructing the geodynamic evolution of the Carpathian area. According to global (Ziegler, 1988; Dercourt et al., 1990; Neugebauer et al., 2001) and regional (Sandulescu, 1994; Csontos, 1995; Dal Piaz et al., 1995; Schmid et al., 1998; Zacher and Lupu,1998) reconstructions of the Mesozoic Tethys, two main oceanic basins were present in the Late Jurassic. To the west, the Ligure-Piemontese oceanic domain and its Penninic northern branch already existed as a narrow, elongated basin between the Western Europe/Iberia and Adria plates, while to the east, Mesozoic Tethys was characterized by a wide oceanic domain (i.e., the Vardar oceanic basin) located between the Adria and the European plates, which in the Late Jurassic was affected by convergence leading to subduction and obduction of the oceanic lithosphere. The connection between the western and eastern domains was represented by a complex area in which the northernmost edge of the Adria

plate was separated from the European plate by small oceanic basins. According to Abbate et al. (1986) and Dal Piaz et al. (1995), this connection was probably characterized by an E-W–trending transfer zone able to accomodate the extension in the Ligure-Piemontese basin, with contemporaneous convergence in the Vardar oceanic domain. Despite the different reconstructions proposed in literature (e.g., Dercourt et al., 1990; Dal Piaz et al., 1995), all authors agree that the Tisza and Alcapa blocks, still joined to the Adria plate in the Late Jurassic, were located in this connection area, in which the oceanic basin represented by the South Apuseni Mountains ophiolites also was situated.

If the South Apuseni Mountains ophiolites were originally located in the northern continuation of the Vardar oceanic domain, as suggested by geological and petrological data presented in this paper, a possible scenario for the Late Jurassic configuration of the Tethys can be drawn (Fig. 13). In this reconstruction the South Apuseni Mountains ophiolites are situated in the Vardar oceanic basin, close to the northernmost edge of the Adria plate. This area was probably characterized by a suprasubduction zone setting where a trapped oceanic crust with MOR affinity was associated to calc-alkaline volcanic sequences, most likely representative of a magmatic island arc (Fig. 13).

According to Dercourt et al. (1990) and references therein, the convergence in the Vardar oceanic basin began in the Middle Jurassic. During Late Jurassic–Early Cretaceous time, this convergence led to the emplacement of Jurassic ophiolites, including the South Apuseni Mountains ophiolites and associated orogenic magmatic sequences. These ophiolites were emplaced with westward vergence, resulting in the large-scale obduction of oceanic slices onto the continental margin of the Adria plate. In the Late Cretaceous–Early Tertiary, this convergence resulted in a massive continental collision, mainly driven by the relative northward motion of the Adria plate with respect to the stable European continental plate. In the Early Tertiary, the deformation was probably intracontinental, although some oceanic domains may still have been opened during Late Eocene time (Schmid et al., 1998, Linzer et al., 1998; Neugebauer et al., 2001). During this convergence, the Tisza and Alcapa blocks probably represented two separate microplates, which subsequently rotated and translated independently (see, for example, the reconstructions of Csontos, 1995 and Neugebauer et al., 2001). In this frame-
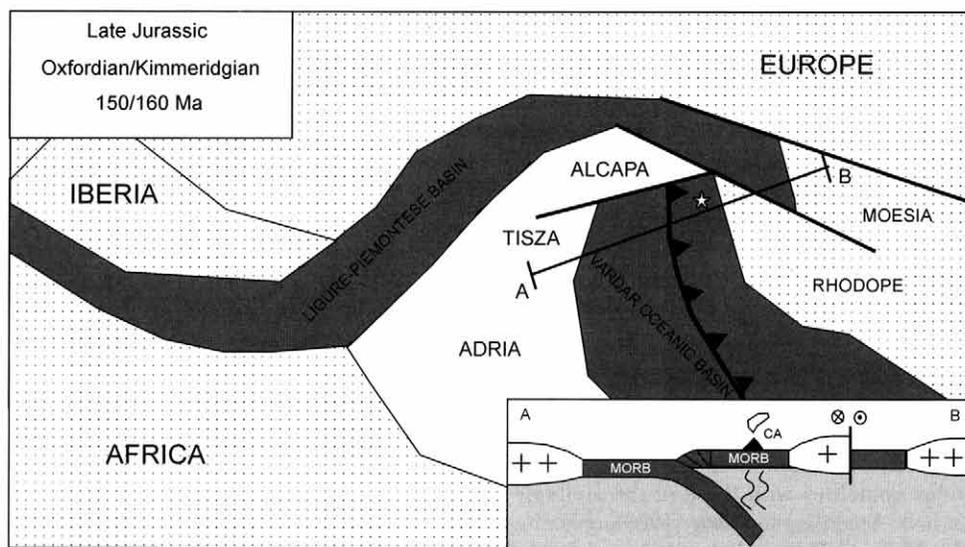
FIG. 13. Tentative Late Jurassic geodynamic reconstruction of the connection between the Ligure-Piemontese and Vardar oceanic basins during the Late Jurassic. The star indicates the probable location of the South Apuseni Mountains ophiolites.

work, the Tisza microplate was derived from the northernmost edge of the Adria plate, and was affected by Jurassic–Cretaceous shortening events (Neugebauer et al., 2001). This area was characterized by a stack of continental and oceanic tectonic units derived from the Adria continental margin and the neighboring Vardar basin, with the latter represented by the South Apuseni Mountains ophiolites and associated island-arc magmatic sequences. In the Late Paleogene–Early Neogene, increased convergence between the Adria and Eastern European plates led to the present-day location of the South Apuseni Mountains ophiolites. This complex tectonic evolution resulted in a large-scale translation of the South Apuseni Mountains ophiolites from their original position at the northern edge of the Vardar zone to their present-day location in the inner zone of the Carpathian belt (Fig. 14); this evolution implies an eastward translation of about 300 km.

This reconstruction fits very well with the escape tectonics models proposed for the Carpathian belt by Csontos (1995), Linzer et al. (1998) and Neugebauer et al. (2001). These models suggest that the continuous convergence from the Cretaceous to Neogene between the Adria and the European plates produced shortening and thickening in the Alpine and Northern Carpathian belts. The upper Paleogene–lower Neogene shortening also was accommodated by the transpressive tectonics connected with the eastward escape of rigid blocks, such as the Alcapa and Tisza microplates, toward the Carpathian belt. This escape was made possible by major strike-slip and/or transpressive faults, such as the Mid-Hungarian line or the south Transylvanian fault system, translating the more rigid blocks toward areas where space was available. According to Csontos (1995), the escape of the Tisza microplate was probably combined with the retreat of the subducting European margin and coeval extension in the Pannonian basin. In this context, the present-day NE-SW structural trend of the South Apuseni Mountains ophiolites was probably acquired not only by displacement, but also by a clockwise rotation of ~90° of the Tisza microplate, as suggested by the paleomagnetic data (Patrascu et al., 1994).

## Conclusions

Unlike reconstructions proposed thus far (e.g., Dal Piaz et al., 1995), the data presented in this paper highlight the occurrence in the South Apuseni Mountains of Middle Jurassic ophiolites, showing mid-oceanic ridge affinity, overlain by an Upper
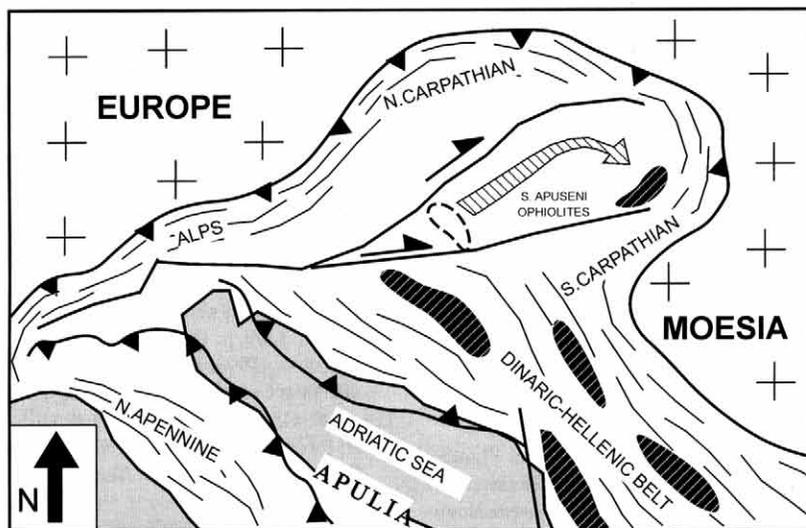
FIG. 14. Sketch of the tectonic setting of the Alpine-Carpathian areas. The probable trajectory of the South Apuseni Mountains during the Neogene is indicated. Strike-slip faults that bounded the Tisza block are also shown.

Jurassic island-arc calc-alkaline magmatic sequences. Our reconstruction suggests that the Late Jurassic geodynamic framework of the South Apuseni Mountains was characterized by MOR oceanic lithosphere trapped in a supra-subduction zone, where calc-alkaline volcanics developed over the previously emplaced oceanic lithosphere.

The geological and petrological data for the South Apuseni Mountains ophiolites suggest that their original location was at the northernmost edge of the Vardar oceanic basin. During the Late Jurassic, these ophiolites were probably emplaced onto the continental margin of the Tisza microplate, which in turn can be considered as the northernmost edge of the Adria plate.

The present-day location of the South Apuseni Mountains on the internal side of the Carpathian belt was reached during the Late Paleogene–Early Neogene, when convergence between the Adria microplate and Eastern European plate produced shortening and thickening in the Alpine and northern Carpathian belts, as well as transpressive tectonics connected with the eastward escape and rotation of the Alcapa and Tisza rigid blocks. Escape tectonics resulted in an eastward motion of the Tisza microplate, leading to the present-day location of the South Apuseni Mountains ophiolites, which are displaced about 300 km eastward with respect to the northernmost Vardar ophiolites.

## REFERENCES

Abbate, E., Bortolotti, V., and Principi, G., 1980, Apennine ophiolites: A peculiar oceanic crust, in Rocci, G., ed., Special issue on Tethyan ophiolites: Ofioliti, v. 1, western area, p.59–96.

Abbate, E., Bortolotti, V., Conti, M., Marcucci, M., Principi, G., Passerini, P., and Treves, B., 1986, Apennines and Alps ophiolites and the evolution of the western Tethys: Memorie della Società Geologica Italiana, v.31, p. 23–44.

Aignes-Torres, M., and Koller, F., 1999, Nature of the magma source of the Szarvasko complex (NE Hungary): Petrological and geochemical constraints: Ofioliti, v. 24, p. 1–12.

Bebien, J., Baroz, F., Capedri, S., and Venturelli, G., 1987, Magmatismes basiques associes à l'overture d'un bassin marginal dans les Hellenides internes au Jurassique: Ofioliti, v.12, p. 53–70.

Bleahu, M., Lupu, M., Patrulius, D., Bordea, L., Stefan, A., and Panin, S., 1981, Guide to the excursion, B3:

Structures of the Apuseni Mts: Bucharest, Romania, Carpatho-Balkan Geological Association XII Congress, 80 p.

Bleahu, M., Soroiu, M., Catilina, R., 1984, On the Cretaceous tectono-magmatic evolution of the Apuseni Mountains as revealed by K-Ar dating: Review of Roumanian Geology, Geophysics, and Geography, v.29, p.123–130.

Briqueu, L., Bougault, H., and Joron, J. L., 1984, Quantifications of Nb, Ta, Ti, and V anomalies in magma associated with subduction zones: Petrogenetic implications: Earth and Planetary Science Letters, v. 68, p. 297–308.

Burchfiel, B. C., 1980, Eastern European alpine system and the Carpathian orocline as an example of collision tectonics: Tectonophysics, v. 63, p. 31–61.

Cioflica, G., Lupu, M., Nicolae, I., Lupu, M., and Vlad, S., 1981, Guide to excursion A3: Alpine ophiolitic complexes in south Carpathian and south Apuseni Mountains: Bucharest, Romania, Carpatho-Balkan Geological Association XII Congress, 80 p.

Csontos, L., 1995, Tertiary tectonic evolution of the intra-carpathian area: A review: Acta Vulcanologica, v. 7, no. 2, p. 1–13.

Dallmeyer, R. D., Pana, D. I., Neibauer, F., and Erdmer, P., 1999, Tectonothermal evolution of the Apuseni Mountains, Romania: Resolution of Variscan versus Alpine events with $^{40}Ar/^{39}Ar$ ages: Journal of Geology, v. 107, p. 329–352.

Dal Piaz, G. V., Martin, S., Villa, I. M., and Gosso, G., 1995, Late Jurassic blueschist facies pebbles from the Western Carpathians orogenic wedge and paleostructural implications for Western Tethys evolution: Tectonics, v. 14, p. 874–885.

Danelian, T., Robertson, A. H. F., and Dimitriadis, S., 1996, Age and significance of radiolarian sediments within basic extrusive of the marginal basin Guevgueli Ophiolite (northern Greece): Geological Magazine, v. 133, p. 127–136.

Dercourt, J., Ricou, L. E., Adamia, S., Csazsar, G., Funk, H., Lefeld, J., Rakus, M., Sandulescu, M., Tollman, A., and Tchoumachenko, P., 1990, Anisian to Oligocene paleogeography of the European margin of Tethys (Geneva to Baku): Memoires de la Societè Géologique de France., v. 154, no. 3, p. 159–190.

Franzini, M., 1979, Analisi chimica di minerali e rocce per spettrometria dei raggi X: Rendiconti della Società Italiana di Mineralogia e Petrografia, v. 35, no. 2, p. 493–506.

Herz, N., and Savu, H., 1974, Plate tectonic history of Romania: Geological Society of America Bulletin, v. 85, p. 1429–1444.

Ivanov, T., Misar, Z., Bowes, D. R., Dudek, A., Dumurdzanov, N., Jaros, J. J., Elinek, E., and Pacesova, M., 1987, The Demir Kapija-Gevgelija ophiolite massif, Macedonia, Yugoslavia: Ofioliti, v.12, p. 457–478.

Horvath, F., and Royden, L., 1981, Mechanism for the formation of the intra-Carpathian basins: A review: Earth Evolutionary Science, v. 3, p. 307–316.

Kovacs, S., 1982, Problems of the "Pannonian Median Massif" and the plate tectonic concept. Contribution based on the distribution of Late Paleozoic–Early Mesozoic isotopic zones: Geologische Rundschau, v. 71, p. 617–640.

Leterrier, J., Maury, R. C., Thonon, P., Girard, D., and Marchal, M., 1982, Clinopyroxene composition as a method of identification of the magmatic affinities of paleo-volcanic series: Earth and Planetary Science Letters, v. 59, p. 139–154.

Linzer, H. G., 1996, Kinematics of retreating subduction along the Carpathian area: Geology, v. 24, p. 167–170.

Linzer, H. G., Frisch, W., Zweigel, P., Girbacea, R., Hann, H. P., and Moser, F., 1998, Kinematic evolution of the Romanian Carpathians: Tectonophysics, v. 297, p. 133–156.

Lugovic, B., Altherr, R., Raczek, I., Hofmann A. W., and Majer, V., 1991, Geochemistry of peridotites and mafic igneous rocks from the Central Dinaric Ophiolite Belt, Yugoslavia: Contributions to Mineralogy and Petrology, v. 106, p. 201–216.

Lupu, M., 1976, The main tectonic features of the Southern Apuseni Mts.: Review of Roumanian Geology, Geophysics, and Geography, v. 25, p. 19–29.

————, 1983, The Mesozoic history of the South Apuseni Mountains: Annales Istitutul Geologie si Geofizica, v. 60, p. 115–124.

Lupu, M., Antonescu, E., Avram, E., Dumitrica, P., and Nicolae, I., 1995, Comments on the age of some ophiolites from the north Drocea Mts: Romanian Journal of Tectonics and Regional Geology, v. 76, p. 21–25.

Marton, E., Pagac, P., and Tunyi, I., 1992, Paleomagnetic investigations on late Cretaceous–Cenozoic sediments from the NW part of the Pannonian basin: Geologica Carphatica, v. 43, p. 363–369.

Miyashiro, A., 1974, Volcanic rock series in island arcs and active continental margins: American Journal of Science, v. 274, p. 321–355.

Neugebauer, J., Greiner, B., and Appel, E., 2001, Kinematics of the Alpine–West Carpathian orogen and paleogeographic implications: Journal of the Geological Society of London, v. 158, p. 97–110.

Nicolae, I., 1995, Tectonic setting of the ophiolites from the South Apuseni Mountains: Magmatic arc and marginal basin: Journal of Tectonics and Regional Geology, v. 76, p. 27–38.

Nicolae, I., Cuna, S., and Soroiu, M., 1987, Preliminary K-Ar investigations of ophiolites from the South Apuseni Mountains (Romania): Stud. cerc: Geologie, Geofizica, Geografia si Geofizica, v. 25, p. 43–49.

Nicolae, I., Soroiu, M., and Bonhomme, G. M., 1992, Ages K-Ar de quelques ophiolites des Monts Apuseni du sud (Roumanie) et leur signification géologique: Géologie Alpine, v. 68, p. 77–83.

Ottonello, G., Joron, J. L., and Piccardo, G.B., 1984, Rare earth and 3d transition element geochemistry of peridotitic rocks: II. Ligurian peridotites and associated basalts: Journal of Petrology, v.25, p. 373–393.

Pamic, J., 1983, Considerations on the boundary between hazburgite and lherzolite subprovinces in the Dinarides and northern Hellenides: Ofioliti, v. 14, p. 3–32.

Pana, D. I., 1998, Petrogenesis and tectonic of the basement rocks of the Apuseni Mountains: Significance for the alpine tectonic of the Carpathian-Pannonian region: Unpubl. Ph.D. thesis, Department of Earth and Atmospheric Science, University of Alberta, Edmonton, 356 p.

Patrascu, S., Panaiotu, C., Seclaman, M., and Panaiotu, C. E., 1994, Timing of rotational motion of Apuseni Mountains (Romania): Paleomagnetic data from Tertiary magmatic rocks: Tectonophysics, v. 233, p.163–176.

Pearce, J. A., 1983, Role of the sub-continenetal lithosphere in magma genesis at active continental margin, *in* Hawkesworth, C. J., and Norry, M. J., eds., Nantwich, UK, Shiva Publ. Co., p. 230–249.

Ratschbacher, L., Linzer, H. G., and Moser, F., 1993, Cretaceous to Miocene thrusting and wrenching along the Central South Carpathians due to a corner effect during collision and orocline formation: Tectonics, v. 12, p. 855–873.

Radulescu, D., and Sandulescu, M., 1973, The plate tectonic concept and the geological structures of the Carpathians: Tectonophysics, v. 16, p. 155–161.

Robertson, A. H. F., 1994, Role of the tectonic facies concept in orogenic analysis and its application to Tethys in the Eastern Mediterranean region: Earth Science Reviews, v. 37, p. 139–213.

Royden, L., 1993, Evolution of retreating subduction boundaries formed during continental collision: Tectonics, v. 12, p. 629–638.

Sandulescu, M., 1984, Geotectonica Romaniei: Bucharest, Romania, Edit. Tehn., 336 p.

———, 1994, Overview on the Romanian geology: Romanian Journal of Tectonics and Regional Geology, v. 75, p. 3–15.

Schmid, S. M., Berza, T. , Vlad, D., Froitzheim, N., and Fugenschuh, B., 1998, Orogen-parallel extension in the Southern Carpathians: Tectonophysics, v. 297, p. 209–228.

Serri, G., 1981, The petrochemistry of ophiolite gabbroic complexes: A key for the classification of ophiolites into low-Ti and high-Ti types: Earth and Planetary Science Letters, v. 52, p. 203–212.

Shervais, J. W., 1982, Ti-V plots and the petrogenesis of modern ophiolitic lavas: Earth and Planetary Science Letters, v. 59, p. 101–118.

Sun, S. S., and McDonough, W. F., 1989, Chemical and isotopic systematics of ocean basalts: Implications for mantle composition and processes, *in* Saunders, A. D., and Norry, M. J., eds., Magmatism in the ocean basins: Geological Society of London, Special Pubblication, v. 42, p. 313–346,.

Trubelja, F., Marchig, V., Burgath, K. P., and Vujovic, Z., 1995, Origin of the Jurassic Tethyan ophiolites in Bosnia: A geochemical approach to tectonic setting: Geologica Croatica, v. 48, no. 1, p. 49–66.

Venturelli, G., Thorpe, R. S., and Potts, P. J.,1981, Rare earth and trace element characteristics of ophiolitic metabasalts from the Alpine-Apennine belt: Earth and Planetary Science Letters, v. 53, p. 109–123.

Zacher, W., and Lupu, M., 1998, The ocean floor puzzle of the Alpine: Carpathian orogenic belt: Jahrbuch der Geologischen Bundesanstalt, v. 141, p. 97–106.

Ziegler, P. A., 1988, Evolution of the Arctic–North Atlantic and the Western Tethys: American Association of Petroleum Geologists, Memoirs, v. 43, p. 1–198.